Rheology of Bitumen Modified by EVA—Organoclay Nanocomposites

Subramanian Sureshkumar Markanday,[1] Jiri Stastna,[2] Giovanni Polacco,[1] Sara Filippi,[1] Igor Kazatchkov,[2] Ludovit Zanzotto[2]

[1]*Dipartimento di Ingegneria Chimica, Chimica Industriale e Scienza dei Materiali (DICCISM), Università di Pisa, Largo LucioLazzarino 2, Pisa 56122, Italy*
[2]*Bituminous Materials Chair, Schulich School of Engineering, University of Calgary, 2500 University Drive NW, Calgary T2N 1N4, Alberta, Canada*

Received 15 September 2009; accepted 27 February 2010
DOI 10.1002/app.32373
Published online 21 May 2010 in Wiley InterScience (www.interscience.wiley.com).

ABSTRACT: Ternary systems, bitumen/ethylene-vinyl acetate (EVA)/organoclay, were prepared by two mixing methods (physical mixing and melt blending) and then studied in small amplitude oscillations, start-up of shear flow and repeated creep and recovery tests. The effect of mixing method and the role of two organoclays on the rheological properties of the studied systems were investigated. Improved thermomechanical properties of bitumen/EVA/organoclay nanocomposites, prepared by melt blending, were demonstrated by the low accumulated strain/compliance in the repeated creep and recovery tests. Structural differences between the studied systems were reflected in the behavior of the dynamic phase angle, specifically in the shape of the derivative of phase angle w.r.t. the reduced frequency. Similarly, the structural differences between the prepared nanocomposites were reflected by the behavior of the stress growth function η^+ in the transient experiments. © 2010 Wiley Periodicals, Inc. J Appl Polym Sci 118: 557–565, 2010

Key words: bitumen; modification; nanocomposites; rheology

INTRODUCTION

Bitumens are chemically complex materials consisting of many thousands of chemical species ranging from nonpolar fully saturated alkenes to highly polar hetero-hydrocarbons.[1] The chemical composition of bitumens cannot be defined exactly, and therefore, their components are usually grouped into asphaltenes and maltenes. The maltenes can be subdivided into saturates, aromatics, and resins. No sudden transition in molecular structure, has been found between resins and asphaltenes.[2,3] The size of asphaltene and resin molecules is not very different[4,5] and whether a particular molecule behaves as an asphaltene or resin depends on various external and internal conditions, such as temperature, pressure, surrounding molecules and so forth. From the practical point of view, bitumens were historically, and still, are used as water proofing and binding materials. Today a huge amount of asphaltic bitumens is used by the paving industry due to their good adhesion to mineral aggregates and their viscoelastic properties. Because of the increasing load as well as the frequency of traffic, the distresses on bituminous binders are more severe and to improve their performance they are frequently modified by various polymers, see, for example, Ref. 6 and the references used therein. The polymers used as modifiers of bituminous binders are: thermoplastic elastomers, plastomers, and reactive polymers.[6] The best performing bituminous binders were obtained by blending conventional bitumens with styrene-butadiene-styrene (SBS) block copolymer or ethylene-vinyl acetate (EVA) copolymer.[6,7] Recently, polymer-layered silicate nanocomposites attracted the attention of material scientists and engineers as a new class of materials. These new materials have vastly improved physical properties even at very low concentration of silicate "fillers". Rheological properties of asphaltic bitumen modified by EVA-layered silicate nanocomposites are studied in this contribution.

Ternary systems of bitumen/polymer/clay, here called polymer-modified asphalt nanocomposites (PMAN) represent a new generation of modifiers for paving bituminous binders. Such materials have to be thoroughly investigated before their prospective introduction into the paving industry.

The incorporation of layered silicates into polymer matrices is not a new topic.[8,9] The renewed interest in polymer-layered silicate nanocomposites dates back to 1985 when the Toyota research group showed that a small amount of layered silicate

Correspondence to: G. Polacco (g.polacco@diccism.ing.unipi.it).

Contract grant sponsors: Natural Sciences and Engineering Council of Canada, Husky Energy Inc.

loaded into Nylon-6 resulted in significant improvement of thermomechanical properties.[10] The next important step was the observation that it is possible to melt-mix polymers with layered silicates without the use of organic solvents.[11] After sufficient mobility of polymer chains is reached, the chains can diffuse into the silicate clay galleries thus producing a new polymer-silicate structure. To achieve the miscibility of layered silicates with a large number of polymers a normally hydrophilic silicate surface has to be converted to an organophilic one. This can be achieved by ion-exchange reactions with cationic surfactants.[12–14] Obviously one cannot obtain a nanocomposite by simple mixing of polymer and silicate (or generally any inorganic material). In such systems, the interaction of organic and inorganic components is weak and thus reflected in poor mechanical properties. When particle agglomeration occurs these systems might have further reduced strength.[15] Depending on the strength of interfacial interaction between the polymer matrix and the layered silicate, two types of nanocomposites can be obtained: (a) intercalated structures where a single (or more) polymer chain is inserted between silicate layers; (b) exfoliated (delaminated) structures, where the clay layers are separated and individually dispersed in the continuum matrix.[15–18] Intercalation results in well ordered multilayer structures of alternating polymeric and silicate layers with a separation distance less than 20–30 Å.[15,16] In delaminated structures the polymer separates the silicate platelets by 80–100Å or more.[15,16]

The exfoliation maximizes the polymer-clay interactions and thus should yield the most significant changes in the physical properties of such systems. It is difficult to achieve complete exfoliation of clays and most of the polymer nanocomposites will have intercalated or mixed (intercalated-exfoliated) nanostructures.[17]

There are only a few studies of ternary systems bitumen/polymer/clay, that is, bitumens modified by polymer-layered silicate nanocomposites. SBS premixed with kaolinite and organobentonite, respectively, were used as modifiers of conventional bitumen in Refs. 19 and 20. SBS premixed with kaolinite was used as modifier of bitumen in Ref. 21. Preparation and properties of asphalt modified by montmorillonite organoclay were studied in Ref. 22. Rheological properties of the bitumen/SBS/Cloisite20A system were studied in Ref. 23. It was shown that intercalation and the glass transition domain were not affected by the mixing procedures. On the other hand, important differences were observed in the rheological behavior of these ternary systems. The two systems, bitumen/Cloisite15A and bitumen/nanofil15 were studied in Ref. 24. The authors claimed that the bitumen used was able to intercalate and partially exfoliate the organoclays. It was also concluded that the elasticity (storage modulus G') of the modified bitumen was higher than in the virgin bitumen, while the loss modulus (G'') was much lower in the modified binder than in the virgin binder.

MATERIALS AND METHODS

EVA copolymer containing 28% (by weight) of vinyl acetate and two types of clays were used to modify a base (conventional) bitumen of 50/70 Pen grade. Two different organoclays were used for the preparation of nanocomposites; Cloisite20A referred to as CL, from Southern Products, USA and Dellite43B, referred to as DL, from Laviosa Chimica Mineraria, Italy. Both clays were derived from a naturally occurring montmorillonite. CL was modified by dimethyldihydrogenated-tallow ammonium chloride and had the following particle size distribution: 2% by weight were below 2 μm, 50% were below 6 μm, and 90% were below 13 μm). DL was modified by dimethyldihydrogenated-tallow ammonium chloride and had an average particle size of 7–9 μm.

From the base bitumen, referred to as B, polymer modified bitumens with 3% EVA (by weight) and 6% EVA (by weight) were prepared. These are referred to as 3*M* and 6*M*. The EVA-clay nanocomposites, with weight ratio always set to 3/2, were prepared by the two different blending methods. In ternary systems B/EVA/clay the first method used physical mixing (PM) in which the polymer and clay were added separately to the base bitumen during the modification procedure. The second method used EVA/clay nanocomposites prepared by melt blending (MB) in the modification process of the base bitumen. The EVA/clay blends were prepared by melt compounding in a Brabender Plasticorder static mixer, preheated to 190°C (CL) and 120°C (DL). The organoclay was added to the molten polymer before increasing the rotor speed. After the extraction from the mixer the samples were cooled naturally in the atmosphere. The blends were then pressed into sheets at temperature of 120°C. After cooling for 3 h, the sheets were cut into uniform chips. The details of the outlined methods are given in Ref. 25. The complete list of the studied systems is given in Table I.

All the materials were subjected to the following rheological tests:

(a). Small amplitude oscillations in a TA-ARES LS2-M rheometer (strain control mode);
(b). Stress growth after initiation of a constant shear rate (start-up experiment);
(c). Repeated creep and recovery (sometimes referred to as the dynamic creep) in a CVOR 200-Malvern rheometer (stress control mode).

TABLE I
Composition and Preparation Method of the Mixtures

System	EVA (wt %)	CL (wt %)	DL (wt %)	Method
B	0	0	0	–
3M	3	0	0	–
6M	6	0	0	–
3M2DP	3	0	2	PM
3M2DB	3	0	2	MB
3M2CP	3	2	0	PM
3M2CB	3	2	0	MB
6M4DP	6	0	4	PM
6M4DB	6	0	4	MB
6M4CP	6	4	0	PM
6M4CB	6	4	0	MB

Tests (a) were performed in the parallel plate geometry (plates of diameter 10, 25, and 50 mm) and in the torsion bar geometry, depending on the temperatures used. Isothermal oscillations (frequency $\tilde{\omega}$ ranging from 0.1 to 100 rad/s) at temperatures from −20 to 70°C were performed and the master curves of dynamic material functions (G', G'', tanδ) were constructed in the software platform IRIS.[26,27] The time temperature shifting was possible for all the studied systems however, a vertical shifting factor had to be applied. Tests (b) were done in cone and plate geometry (diameter 25mm and cone angle 0.1 rad) at fixed temperature $T = 60$°C and shear rates varying from 0.5 to 5 s^{-1}. The repeated creep and recovery tests were performed in plate-plate geometry (25 mm diameter) and $T = 40$°C. One hundred cycles of 1 s creep and 9 s recovery were studied with the applied shear stress of 100 Pa. Both tests (a) and (c) were performed in the linear viscoelastic domain. The strains in test (b) were high enough to reach the nonlinear behavior of some of the systems studied.

The full characterization of the chemistry and morphology of the prepared mixes is given in Ref. 25. Briefly, the morphological analysis showed that at high polymer concentrations the presence of the clay favored the dispersion of polymer in the asphalt matrix. However, both the type of clay and the method of clay addition affected the final properties. In particular, CL had a significant compatibilizing effect on the asphalt/polymer interactions. This was explained by the X-ray diffraction, which showed that: (1) CL, with respect to DL, had a higher affinity with the polymer; (2) in PM the clays were mainly intercalated by the asphalt molecules, while in MB the preformed interactions between clay and polymer survived the process of mixing with asphalt. The two clays acted as compatibilizers that increased the interactions between asphalt and polymer. The higher the clay/polymer affinity, the stronger was this effect. Therefore, the homogeneity in morphology increased from asphalt/polymer to asphalt/polymer/dellite, and then to asphalt/polymer/cloisite.

RESULTS AND DISCUSSION

Dynamic material functions and structural characteristics

The addition of clay did not reveal dramatic changes in the behavior of the master curves of storage and loss moduli of the studied modified bitumens. Based on the linear viscoelastic behavior of G' and G'' all systems resembled amorphous polymeric systems of low molecular weight.[26,28] Generally, the values of both dynamic moduli, in modified systems, were higher than in the base bitumen. As the master curves of the dynamic material functions (reference temperature $T_r = 0$°C) cover the temperature interval −20/70°C, the "master" loss moduli displayed a strong (absolute) maximum at high reduced frequencies ($\omega = a_T\tilde{\omega}$).

On the other hand, none of the master storage moduli, G', showed the plateau modulus, G_N^0. Only an inflection point can be identified on master curves of G'. To distinguish the studied systems one has to use some more exotic linear viscoelastic plot. In Ref. 23, the modified loss tangent function [tan$c(\delta) = (J'' - 1/\omega\eta_0)/J'$), where η_0 is the zero-shear viscosity] was successfully used to achieve this goal. Another possibility is to use the so called Van Gurp–Palmen plot.[29] A Van Gurp–Palmen (vGP-plot) is the plot of the phase angle versus the magnitude of the complex modulus $|G^*|$ and it was originally proposed as a tool for the verification of the time superposition principle.[29] This plot is also known under the name Black diagram.[30] In Ref. 31, the method of van Gurp and Palmen was used for the identification of polydispersity and long chain

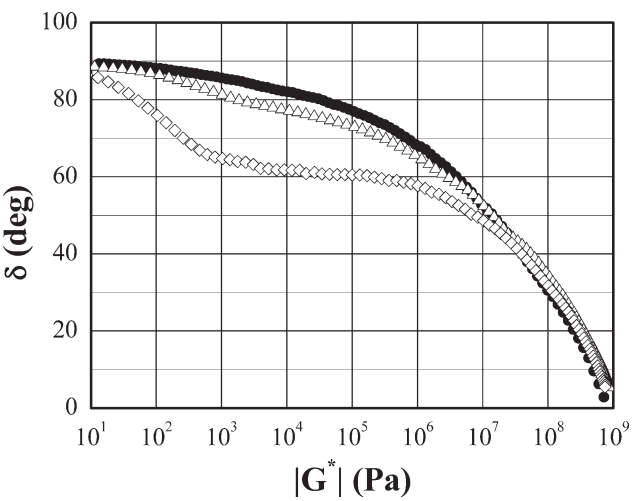

Figure 1 The Van Gurp–Palmen plots, Tr = 0°C. ● B, Δ 3M, ◇ 6M.

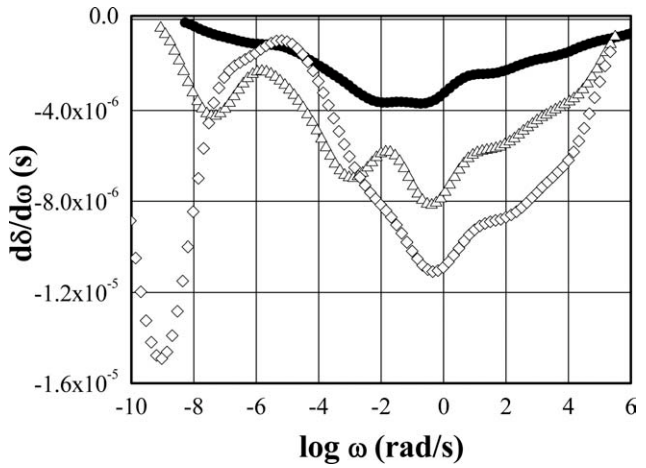

Figure 2 Derivative of phase angle, Tr = 0 C. ● B (magnitude multiplied by 8), Δ 3M, ◇ 6M.

branching in polymer melts. Figure 1 is a vGP-plot for systems B, 3M, and 6M. It is clear that the absence of the pronounced plateau modulus yields a smooth vGP-plot for each of these systems and similarly no characteristic minimum can be observed for either of the studied systems.

Similar vGP-plots can be constructed for the rest of the studied systems (base bitumen modified by EVA organoclay nanocomposites). The main difference apparent from such plots is the clear split between materials with 3 and 6% wt EVA. A better chance to illuminate the differences in the composition or/and the method of preparation of the studied materials would have the derivative of the phase angle w.r.t. the reduced frequency ω. Figure 2 shows $d\delta/d\omega$ for the base bitumen (B) and its modifications 3M and 6M. The rates of change of the phase angle were negative in all three systems, that is, the phase angle is monotonically decreasing from $\pi/2$ to 0 with increasing ω. The magnitude of the rate of change of δ is much smaller in B than in 3M and 6M. The characteristic peak in B is positioned roughly between $\omega \sim 0.01$ and 1 rad/s. This peak splits into a wave form in 3M and then changed into a symmetric peak in the 6M system. A shoulder at $\omega < 100$ rad/s is basically preserved in all three systems.

The domain $\omega < 0.01$ rad/s is populated with several changes in the systems 3M and 6M. A small shoulder at $\omega < 10^{-5}$ rad/s (visible only in "magnification") in base bitumen B disappeared in 3M and exists in much weaker form in 6M as a part of a broad peak centered at $\omega \sim 10^{-5}$ rad/s. The system 3M shows a principal maximum at the same frequency. Left of this maximum the clear minima, in both 3M and 6M, are seen. The minimum in 6M (at $\omega \sim 10^{-9}$ rad/s) is of much larger magnitude than that in 3M ($\omega \sim 10^{-7}$ rad/s). Systems containing the clay DL and prepared by both methods (PM and

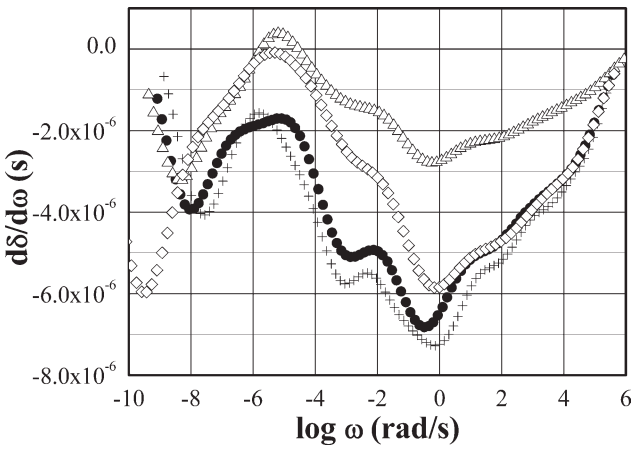

Figure 3 Derivative of phase angle, Tr = 0°C. + 3M2DP, ● 3M2DB, Δ 6M4DP, ◇ 6M4DB.

MB) are depicted in Figure 3. The first noticeable effect is the split into systems containing two different concentrations of EVA copolymer. Generally, the rates of changes of the phase angle are "slower" over a large part of the portrayed ω-domain, in the systems with 6 wt % concentration of EVA.

The shapes of $d\delta/d\omega$ for systems 3M2DP and 3M2DB are remarkably similar except the flat principal maximum peak in 3M2DB (positioned at $\omega \sim 10^{-6}$ rad/s). The central "wavy" part of 3M is still visible in 3M2DP and 3M2DB but with the minimum peak at $\omega \sim 1$ rad/s, and of larger magnitude than in 3M system. The minimum peak of 6M (at $\omega \sim 10^{-9}$ rad/s) is now reflected by the system 6M4DB however, with smaller magnitude. The system 6M4DP shows a minimum peak coinciding with the minimum peak of 3M2DB. The principal maxima peaks of 6M4DP and 6M4DB are quite similar. Both are slightly shifted to the right of the principal maximum peak of 3M and positioned at about the same reduced frequency $\omega \sim 10^{-5}$ rad/s as is the

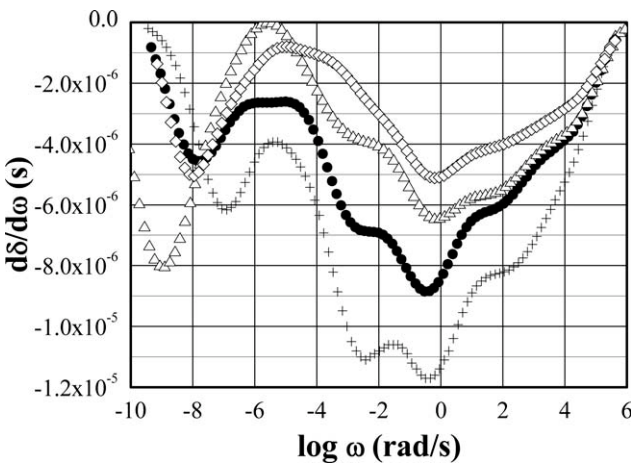

Figure 4 Derivative of phase angle, Tr = 0°C. + 3M2CP, ● 3M2CB, Δ 6M4CP, ◇ 6M4CB.

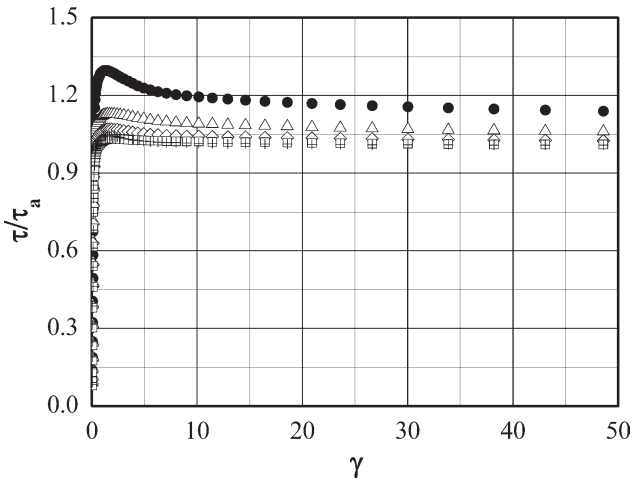

Figure 5 Normalized stress as a function of strain, $T = 60°C$, $\dot{\gamma} = 4\,s^{-1}$. ● 3M2CB, Δ 3M2DB, ◇ 3M2CP, □ 3M2DP, + 3M, (the last two samples are almost indistinguishable).

maximum peak of 6M system. The methods of preparation (systems with clay DL) had a greater impact on the systems with 6% wt of EVA copolymer than on systems with 3% wt EVA, as can be seen over a large part of the ω domain.

Figure 4 is similar to Figure 3, but shows the systems with clay CL. The split into two groups, determined by the concentration of EVA, is again apparent. The previously mentioned "wavy" character of the principal minimum peak is now preserved only in the system 3M2CP.

Remarkable is the flat maximum peak of the system 3M2CB centered at $\omega \sim 10^{-5}$ rad/s. This peak is quite broad but not as flat as in the system 6M4CB. The minimum peak at $\omega \sim 10^{-9}$ rad/s now appears in system 6M4CP and the minimum peak at $\omega \sim 10^{-8}$ rad/s is almost identical in systems 3M2CB and 6M4CP. The latter of these systems also has the "strongest" maximum of all the systems portrayed in Figure 4. From both Figures 3 and 4, one can see the impact of the method of preparation (of nanocomposites) on the modified bitumens.

It seems to be possible to conclude that the information hidden in the phase angle and particularly in its derivative w.r.t. the reduced frequency ω is quite rich and Figures 2–4 show the structural changes in the studied modified systems.

Start-up of steady shear

One of the crucial tests of any theory of viscoelastic behavior of materials is a simple stress growth experiment.[26,32–35] In this test, in polymeric systems, the stresses can reach quite high values before settling to their asymptotic values and the ubiquitous stress-overshoot is observed. Multiple overshoots of the shear stress were observed and discussed in.[32,35,36] Stress overshoots in organoclay nanocomposites were studied in Refs. 37–39 and related to the structure of nanocomposites. We have studied the above described systems in transient shear flows (start-up of steady shear) with several shear rates at constant temperature $T = 60°C$. Similarly, as in dynamic shear experiments, the materials with 3% and 6 wt % EVA formed two distinct groups. This can be seen in Figures 5 and 6. In these figures, the shear stress (τ) normalized by its asymptotic value (τ_a) is plotted versus the strain (γ) for the tests with shear rate $\dot{\gamma} = 4\ s^{-1}$. Much smaller overshoots are observed for the modified bitumens with 3% wt EVA (data for 3M2DP and 3M are almost identical) than for the ones modified by 6% wt EVA. Comparing the magnitudes of τ/τ_a(from the highest to the smallest) the sequence of the tested materials is: 3M2CB, 3M2DB, 3M2CP, 3M2DP, 3M—for systems with 3% wt EVA.

Similarly the sequence for 6% wt EVA materials ($\dot{\gamma} = 4\ s^{-1}$) was: 6M4CB, 6M4CP, 6M4DB, 6M4DP, 6M. Because the 6% wt EVA systems are more clearly distinguishable we are presenting their transient properties in the following figures: Figures 7 and 8 show the stress growth function η^+ in systems 6M4CP and 6M4CB, respectively.

Both systems show typical primary maxima of η^+ and their positions move toward shorter times with increasing applied shear rate. In system 6M4CB the shear rate $\dot{\gamma} = 5\ s^{-1}$ produced unreliable results and this shear rate is not included in Figure 8. Aside from the principal maxima there are weak secondary maxima of η^+, these are more visible at higher shear rates in system 6M4CP. This system approaches the asymptotic steady state value for lower shear rates (0.5, 1, 2 s^{-1}) after 1000s. The values of η^+ are much

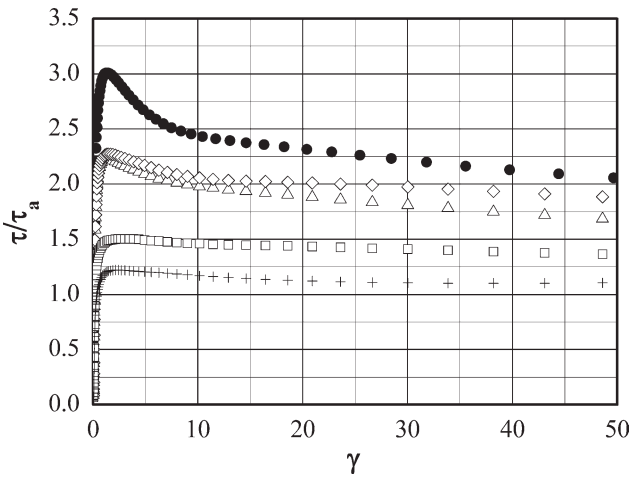

Figure 6 Normalized stress as a function of strain, $T = 60°C$, $\dot{\gamma} = 4\,s^{-1}$. ● 6M4CB, Δ 6M4DB, ◇ 6M4CP, □ 6M4DP, + 6M.

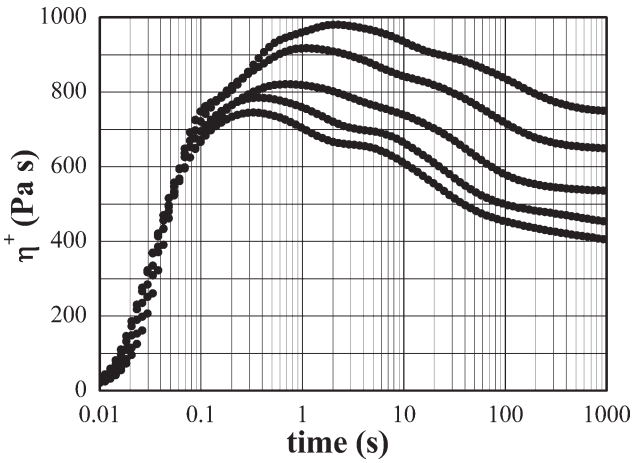

Figure 7 Stress growth function, $T = 60°C$, $\dot{\gamma} = 0.5$, 1, 2, 4, 5 s^{-1} ↓. Modified bitumen 6M4CP.

higher in system 6M4CB and the stress growth function, η^+, is still decreasing after 1000 s. The systems with 6% wt EVA and clay DL are portrayed in Figures 9 and 10. The sample 6M4DP, Figure 9, is reaching the steady state values of η^+ after 1000 s and is also showing weak secondary maxima for the tests at higher values of the shear rate. The values of η^+ were smaller in this system when compared with the system 6M4DB.

The latter system seems to approach the steady state after 1000s for $\dot{\gamma} = 0.5$, 1, 2 s^{-1}. The tests at higher shear rates ($\dot{\gamma} = 4$ and 5 s^{-1}) show η+ still decreasing at $t = 1000$ s. When the transient data are plotted as the shear stress versus the strain, the principal maximum (overshoots of τ) appeared roughly at the same value of the strain γ, see Figure 11 where the system 6M4CB is portrayed ($\gamma_{max} \sim 1.4$).

The magnitude of the overshoot was increasing with the increasing shear rate in all the systems studied. Generally, the stresses generated in the tested modified bitumens were much higher in systems containing the clay CL when the nanocomposites were prepared by the MB method. The discussed transient shear flow was performed up to very high strains, that is, the nonlinear region was reached very quickly and as shown, at least for the systems with 6% wt EVA, one can easily recognize the materials with different clays and prepared by the two discussed methods of preparation.

Repeated creep and recovery

Experiments employing the repetitive loading and unloading are frequently used in the testing of engineering materials.[26,40,41] This type of testing is also applied to samples of paving mix[42] and recently also to the bituminous binders of such mixes.[43–45] All the systems studied in this contribution were subjected to one hundred cycles of shear creep (duration of 1 s) and recovery (9 s of duration).[44,45] The applied stress was 100 Pa, the testing temperature was 40°C and the accumulated compliance $J_{acc}(t)$ was monitored during the experiment. The relatively low level of stress was chosen in order to keep the strain small (linear viscoelastic domain) at least during the first 10–20 cycles. Of course with the increasing number of cycles the strain is increasing and the final accumulated strain can reach high values (depending on the temperature of the test). It is believed that such accumulated strain, in bituminous binders, is responsible for rutting, a very common distress mode in bituminous paving. At higher temperatures the recovery (during the 9s of recovery in one cycle) is usually very small and elastic properties of the tested bitumen are strongly suppressed. At $T = 40°C$, the studied systems, with the exception of the base bitumen B, displayed recovery (viscoelastic behavior) in individual cycles. On the other hand, at this temperature, one can expect the onset of rutting in pavements with this bituminous binder.

The plots of accumulated compliances for the systems B, 3M, and 6M are shown in Figure 12. As expected, the highest values of $J_{acc}(t)$ were attained in the base bitumen and the lowest ones were obtained in 6M. The values of J_{acc} in 3M were between those found in systems B and 6M. The plots for other systems are similar in appearance to those in Figure 12, thus, the individual systems can be graded by the values of J_{acc} attained after 100 cycles of creep and recovery. From high to low values of J_{acc}, the sequence of the 3% wt EVA systems is: 3M2DP, 3M, 3M2CP, 3M2DB, and 3M2CB. The accumulated strain is high in systems with both clays prepared by the PM method. The systems modified by melt blended nanocomposites (DL or CL clays) had a smaller accumulated compliance (i.e., also the

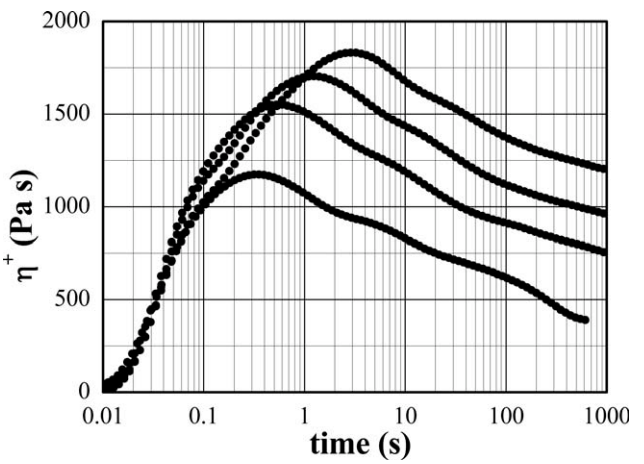

Figure 8 Stress growth function, $T = 60°C$, $\dot{\gamma} = 0.5$, 1, 2, 4 s^{-1} ↓. Modified bitumen 6M4CB.

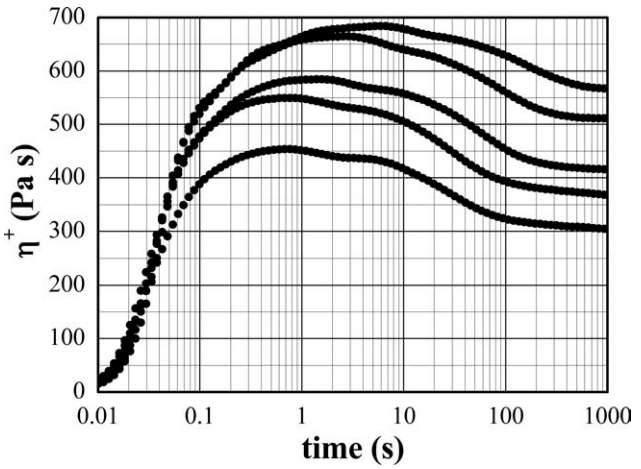

Figure 9 Stress growth function, $T = 60°C$, $\dot{\gamma} = 0.5$, 1, 2, 4, 5 s^{-1} ↓. Modified bitumen 6M4DP.

strain) compared to the base bitumen modified by 3% wt EVA only. The system 3M2CB was best "performing" of all 3% wt EVA materials.

In 6% wt EVA systems the situation was similar. The best "performing" systems were again the materials prepared by MB method with little difference between the two used clays (DL or CL). In samples prepared by PM the clay CL "performed" better (smaller J_{acc}) than clay DL (Table II).

The accumulated compliance function $J_{acc}(t)$ can be described with the help of small number of Voigt elements,[26,44,45] that is, assuming that the shear compliance function $J(t)$ has the form

$$J(t) = J_g + \sum_{i=1}^{N} J_i(1 - e^{-\frac{t}{\Lambda_i}}) + t/\eta_0 \qquad (1)$$

Where N is the number of modes, J_g is the glassy compliance, $\{\Lambda_i, J_{ii}\}$ is the discrete retardation spectrum and η_0 is the zero-shear viscosity.

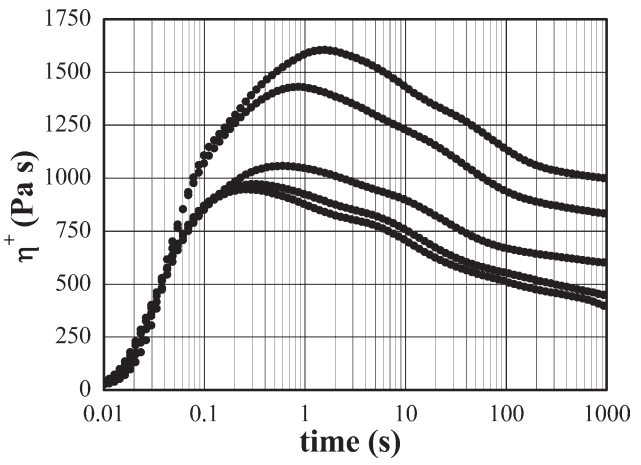

Figure 10 Stress growth function, $T = 60°C$, $\dot{\gamma} = 0.5$, 1, 2, 4, 5 s^{-1} ↓. Modified bitumen 6M4DB.

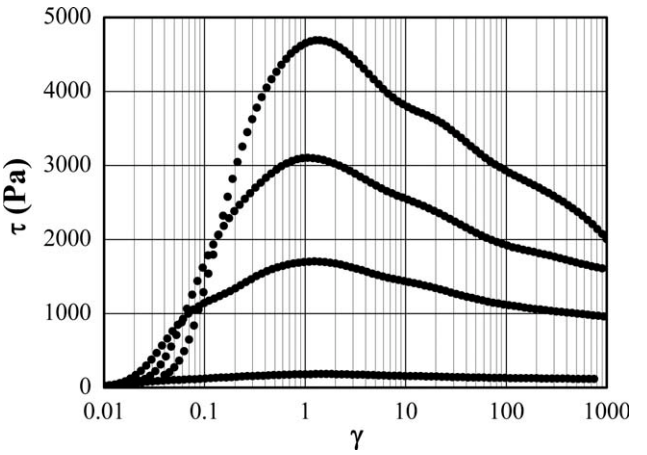

Figure 11 Stress as a function of strain, $T_r = 60°C$, shear rates 4, 2, 1, 0.5 s^{-1} ↓. Modified bitumen 6M4CB.

The fit of $J_{acc}(t)$ for 6M4CB is shown in Figure 13, where $N = 3$. One can see that after first five cycles the compliance function (1) describes the accumulated compliance $J_{acc}(t)$ quite well even with a minimum of retardation modes.

The base bitumen (B) represents the other "end" of the tested materials. This material (at $T = 40°C$) had almost no recovery in individual cycles and thus the viscous approximation of (1) is satisfactory for the description of the repeated creep and recovery test, that is,

$$J(t) = J_e^0 + t/\eta_0 \qquad (2)$$

was suitable for the description of J_{acc} in the base bitumen. J_e^0, in (2) is the steady state compliance. The fit of J_{acc}, for the base bitumen B is given in Figure 14.

The repeated creep and recovery experiment also seems to be able to recognize the individual systems

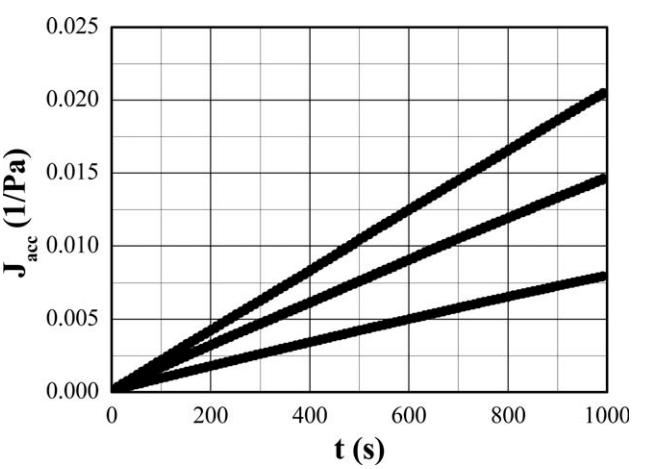

Figure 12 Accumulated creep, Tr = 40 C. Systems B, 3M, 6M ↓.

TABLE II
Accumulated Compliance at $t = 1000$ s, $\tau = 100$ Pa

System	$J_{acc}(1000)$ [1/Pa]
B	0.0205
3M	0.0146
6M	0.00795
3M2DP	0.0188
3M2CP	0.0159
3M2DB	0.0139
3M2CB	0.00711
6M4DP	0.00725
6M4CP	0.00301
6M4DB	0.00205
6M4CB	0.00203

studied in this contribution. Similarly to $d\delta/d\omega$ and η^+ functions, the accumulated compliance J_{acc} divides the materials into two groups according to the concentration of EVA copolymer. Moreover, thanks to the substantial increase of the accumulated strain, this experiment seems to be sensitive to the structural differences between the tested materials.

CONCLUSIONS

From the behavior of the phase angle in the linear viscoelastic domain, it follows that the concentration of EVA copolymer had a strong impact on the rheological properties of the ternary systems B/EVA/clay. The physical method of mixing polymer and clay and subsequent modification of the base bitumen by this mixture produced modified bitumen with a structure that is not so different from the structure of the bitumen modified just by the EVA copolymer. On the other hand, the MB of polymer and clay with subsequent modification of the base bitumen by such nanocomposites produced modified bitumens with structures different from that of

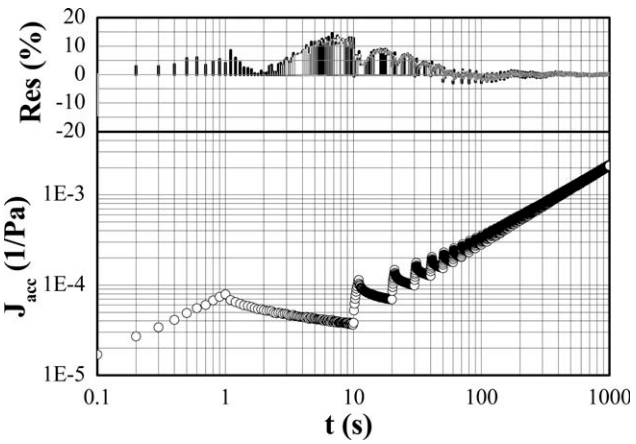

Figure 13 Accumulated compliance in 6M4CB, $T = 40°C$. Fit to eq. (1) (for clarity, the goodness of the fit is identified by the residuals of the fit).

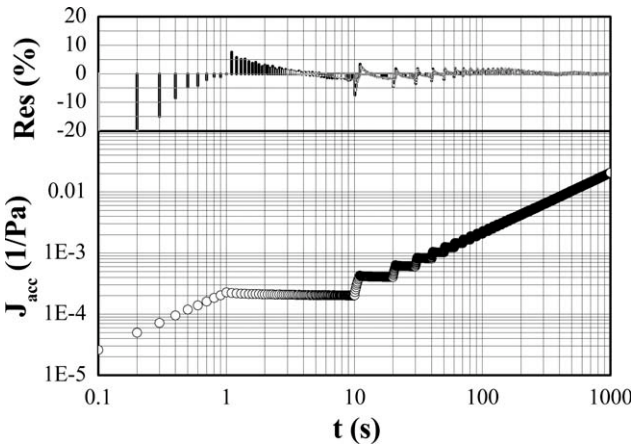

Figure 14 Accumulated compliance in B, $T = 40°C$. Fit to eq. (2) (for clarity, the goodness of the fit is identified by the residuals of the fit).

B/EVA modified bitumen. The experiments in which large strains were used were able to distinguish the individual modified bitumens very easily. Different morphologies of modified bitumens could be identified when the two methods of processing were used (PM or MB). In Refs. 37 and 38, the stress overshoots were attributed to a rupture of the network structure and to particle orientation. In our ternary systems (PMAN), the magnitudes of overshoots and the times where they were observed were strongly dependent on the applied shear rates. The stresses and the overshoots were highest in bitumens modified by clay CL and prepared by the MB method. Similarly, the stresses and overshoots in ternary systems with clay DL were higher when the MB method was used however, with much smaller magnitudes in comparison to the systems with clay CL. Thus, one can assume that the network and exfoliation were strongest in modified bitumen 6M4CB followed by the system 6M4CP. The analogous sequence was followed by systems with clay DL. Similar conclusions can be drawn from the comparison of accumulated creep compliances in the repeated creep and recovery tests. Ternary systems prepared by MB displayed the smallest J_{acc}. The PM of EVA and clay CL produced modified bitumens with much lower values of the accumulated compliance than the same method using clay DL. These conclusions are supported by the results of wide angle X-ray diffraction discussed in Refs. 25 and 46, where it was shown that in PM systems, B/EVA/CL, the intercalated structure was not as coherent as in MB systems. In systems with clay DL, the MB again produced more homogeneous systems than those prepared by PM, however, the surfactant effect of clay DL was not as strong as that of clay CL because DL has weaker affinity for EVA, and thus, part of the polymer did not intercalate this clay.

The authors would like express their gratitude to the Natural Sciences and Engineering Council of Canada and to Husky Energy Inc., for their financial support of this work. Author MSS offers his sincere gratitude to "Leonardo Da Vinci" School of Engineering, University of Pisa, Pisa, Italy for providing funding to carry out this research work through an international Ph.D., Grant.

References

1. Speight, J. G. The Chemistry and Technology of Petroleum; Marcel Dekker: New York, 1999.
2. Groenzin, H.; Mullins, O. C. J Phys Chem A 1999, 103, 11237.
3. Pfeiffer, J. P.; Saal, R. N. J. J Phys Chem 1940, 44, 139.
4. Storm, D. A.; Sheu, E. Y. Fuel 1995, 74, 1140.
5. Porte, G.; Zhou, H. G.; Lazzeri, V. Langmuir 2003, 19, 40.
6. Polacco, G.; Stastna, J.; Biondi, D.; Zanzotto, L. Curr Opi Coll Int Sci 2006, 11, 230.
7. Airey, G. D. Const Build Mat 2002, 16, 473.
8. Cho, J. V.; Paul, D. R. Polymer 2001, 42, 1083.
9. Uskov, I. A. Vysokomol Soed 1960, 2, 926.
10. Sinha Ray, S.; Okamoto, M. Prog Polym Sci 2003, 28, 1539.
11. Vaia, R. A.; Ishhi, H.; Giannelis, E. P. Chem Mater 1993, 5, 1694.
12. Blumstein, A. J Polym Sci A: Polym Chem 1965, 3, 2665.
13. Krishnamoorti, R.; Vaia, R. A.; Giannelis, E. P. Chem Mat 1996, 8, 1728.
14. Ray, S. S.; Bousima, M. Prog Mat Sci 2005, 50, 962.
15. Giannelis, E. P. Adv Mat 1996, 8, 29.
16. Alexandre, M.; Dubois, P. Mat Sci Eng: R 2000, 28, 1.
17. Chin, I. J.; Thurn-Albrecht, T.; Kim, H. C.; Russell, T. P.; Wang, J. Polymer 2001, 42, 5947.
18. Kim, C. M.; Lee, D. H.; Hoffman, B.; Kressler, J.; Stoppelman, G. Polymer 2001, 42, 1095.
19. Ouyang, C.; Wang, S.; Zhang, Y.; Zhang, Y. Polym Degrad Stab 2005, 87, 309.
20. Wang, Y. P.; Liu, D. J.; Wang, Y. P.; Gao, J. M. Polym Polym Comp 2006, 14, 403.
21. Ouyang, C.; Wang, S.; Zhang, Y. Eur Polym J 2006, 42, 446.
22. Jianying, Y.; Zheng, X.; Wu, S.; Liu, G. Mat Sci Eng A 2007, 447, 233.
23. Polacco, G.; Kriz, P.; Filippi, S.; Stastna, J.; Biondi, D.; Zanzotto, L. Eur Polym J 2008, 44, 3512.
24. Jahromi, S. C.; Khodaii, A. Const Build Mat 2009, 23, 2894.
25. Sureshkumar, M. S.; Filippi, S.; Polacco, G.; Kazatchov, I.; Stastna, J.; Zanzotto, L. Eur Polym J 2010, 46, 621.
26. Ferry, J. D. Viscoelastic Properties of Polymers; Wiley: New York, 1980.
27. Mours, M.; Winter, H. H. IRIS Handbook; IRIS Development: Amherst, MA, 2004.
28. Stastna, J.; Zanzotto, L. J Rheol 1999, 43, 719.
29. Van Gurp, M.; Palmen, J. Rheol Bull 1998, 67, 5.
30. Trinkle, S.; Walter, P.; Friedrich, C. Rheol Acta 2002, 41, 103.
31. Marastenau, M. O.; Anderson, D. A. Transp Res Rec 1981, 1766, 32.
32. Osaki, K.; Inoue, T.; Isomura, T. J Polym Sci Part B: Polym Phys 2000, 38, 1917.
33. Osaki, K.; Inoue, T.; Uematsu, T. J Polym Sci Part B: Polym Phys 2000, 38, 3271.
34. Inoue, T.; Yamashita, Y.; Watanabe, H. Macromolecules 2004, 37, 4317.
35. Islam, M. T. Rheol Acta 2006, 45, 1003.
36. Osaki, K.; Watanabe, H.; Inoue, T. Nihon Reoroji Gakaishi 1999, 27, 63.
37. Solomon, M. J.; Almusallam, A. S.; Seefedt, K. F. Macromolecules 2001, 34, 1864.
38. Letwimolnun, W.; Vergnes, B.; Ausias, G.; Carreau, P. J. J Non-Newt Fluid Mech 2007, 141, 167.
39. Vermant, J.; Ceccia, S.; Dolgovskij, K.; Maffettone, P. L.; Macosko, C. W. J Rheol 2007, 51, 429.
40. Payne, A. R.; Kraus, G. Reinforcement of Elastomers; Interscience Publishers: New York, 1965.
41. Song, B.; Chen, W. Exp Mech 2004, 44, 622.
42. Lai, J. S. Highway Res Rec 1973, 468, 73.
43. Bahia, H.; Hanson, D. I.; Zheng, M.; Zhai, H.; Khatri, M. A.; Anderson, R. M. National Cooperative Highway Research Program, Report 459, Washington, DC, 2001.
44. Stastna, J.; Zanzotto, L.; Wasage, T. L. J.; Polacco, G.; Cantù, M. Proc. International Conference on Advanced Characterization of Pavement and Soil Engineering Materials, Loizos, S., Ed. Taylor & Francis Group: Athens, 2007; Vol.1, 303–315.
45. Polacco, G.; Stastna, J.; Zanzotto, L. Rheol Acta 2008, 47, 491.
46. Sureshkumar, M. S.; Filippi, S.; Biondi, D.; Polacco, G. EVA/Asphalt Nanocomposites: Preparation and Properties, Proc. International Conference on Nanotechnology and Advanced Materials (ICNAM-2009), May 3–7; University of Bahrain: Bahrain, 2009; 138.